Arrangement of Conductive TiO_2 Nanoparticles in Hybrid Inorganic/Organic Thermosetting Materials Using Liquid Crystal

Agnieszka Tercjak,* Junkal Gutierrez, Laura Peponi, Lorena Rueda, and Iñaki Mondragon*

Materials + Technologies Group, Departamento de Ingeniería Química y del Medio Ambiente, Escuela Politécnica, Universidad del País Vasco/Euskal Herriko Unibertsitatea, Plaza Europa 1, 20018 Donostia-San Sebastián, Spain

Received October 8, 2008; Revised Manuscript Received March 24, 2009

ABSTRACT: Novel thermoresponsive hybrid inorganic/organic thermosetting materials based on hydrophobic titanium dioxide nanoparticles and amphiphilic poly(styrene-*b*-ethylene oxide) block-copolymer-dispersed 4′-(hexyl)-4-biphenyl carbonitrile liquid crystals were prepared and characterized. The obtained results confirm that these multiphase materials maintain thermo-optical properties of incorporated liquid crystals and show good dispersion of the titanium dioxide, which the microphase separated within the HBC/PS-block. Moreover, well-dispersed nanoparticles spontaneously form well-defined highly dense arrays of titania nanodots located in the interface between the epoxy matrix and the microphase-separated HBC/PS-block, which, combined with the fact that TiO_2 nanoparticles maintain their conductive properties in the investigated systems, can lead to the generation of novel materials with interesting specific properties.

Introduction

The manufacture of metal-based nanoarchitectured materials (such as nanoparticles, nanorods, nanowire, or nanosheets) is currently an active research field because of their potential applications in very wide areas of nanotechnology such as electronics, magnetics, optics, photonics, and electrochemistry or catalysis.[1−6] Special attention is paid to the development of new hybrid inorganic/organic liquid crystal materials because dispersion of the different nanoparticles in low-molecular-weight liquid crystals allows for the design of new liquid crystal devices (LCDs) given that semiconductor nanoparticles dispersed in the liquid crystal or polymer matrix can lead to large electro-optic[7−12] or photorefractive effects.

As is well known, thermosetting blends can be nanostructured by the addition of amphiphilic block copolymers consisting of a thermoset-miscible and thermoset-immiscible block.[13−24] Moreover, recently, Tercjak et al.[25−30] have published a new strategy for the preparation of thermosetting systems modified by block-copolymer-dispersed liquid crystals. In this novel strategy for the preparation of thermo- and electroresponsive materials, amphiphilic block copolymers are used as both a nanostructured agent for epoxy network and a dispersing agent for low-molecular-weight liquid crystals. These novel materials can find application in the field of liquid crystals that possess nematic−isotropic transition and allow the design of materials that can switch from the opaque scattering state to the transparent state because of the matching of the refractive index of the polymer and the oriented LC by applying an external field (electrical, magnetic field, or thermal gradients).

The main aim of the present contribution was to obtain novel hybrid inorganic/organic thermosetting materials on the basis of rutile TiO_2 nanoparticles and 4′-(hexyl)-4-biphenyl-carbonitrile (HBC), low-molecular-weight liquid crystals. The addition of nematic low-molecular-weight liquid crystals to the system allows for the achievement of thermoresponsive materials, and simultaneously, HBC has been used as a dispersing agent for TiO_2 nanoparticles. Titanium dioxide nanoparticles were employed taking into account their conductive and optical properties, which consequently can produce large electro-optic effects on these novel hybrid inorganic/organic thermosetting materials. A small amount of the amphiphilic poly(styrene-*b*-ethylene oxide) block copolymer (PSEO) has been added to the epoxy systems to control both the dispersion of the HBC phase in the PS block and the final morphology generated in the thermosetting system.[26,28−30]

* To whom all correspondence should be addressed. E-mail: scptesza@ehu.es (A.T.); inaki.mondragon@ehu.es (I.M.).

Experimental Part

A diglicydylether of bisphenol A epoxy monomer (DGEBA) (Dow DER 332, gifted by Dow Chemical) was used as reactive solvent. This epoxy network was cured with a stoichiometric amount of an aromatic amine hardener, *m*-xylylenediamine (MXDA), supplied by Sigma-Aldrich. Diblock copolymer of PSEO (Polymer Source) was used as self-assembling agent as well as polymer-dispersed liquid crystal (PDLC). Number-average molecular weights for PS and PEO blocks are 58 600 and 31 000 g mol^{-1}, respectively; the polydispersity index for this copolymer is 1.03. The low-molecular-weight nematic liquid crystal used was 4′-(hexyl)-4-biphenyl carbonitrile (HBC), supplied by Sigma-Aldrich, which was used without further purification. Hydrophobic titanium dioxide nanoparticles (rutile with the crystal size around 20 nm) supplied by Kemira Pigments Oy were used.

Protocol for Blending. TiO_2−PSEO-HBC-(DGEBA/MXDA), TiO_2−PSEO-(DGEBA/MXDA) inorganic/organic thermosetting materials, and epoxy blends modified with PSEO and HBC without TiO_2 nanoparticles were prepared following the same procedure. First, we sonicated 1 wt % TiO_2 nanoparticles in toluene at room temperature by using a microprocessor sonicator 750 W (Vibracell 75043) from Bioblock Scientific with an amplitude range between 20 and 25%. After 2 h, 15 wt % of PSEO block copolymer, 40 wt % of HBC liquid crystal, or both were added and sonicated for an additional 30 min. Then DGEBA epoxy monomer was introduced, and the resultant mixture was heated to 80 °C in an oil bath until complete solvent removal was achieved. To control final morphology, we chose the molar ratio between PSEO and HBC by taking into account our previous work.[26,29,30] Once the solvent was removed, the curing agent, MXDA, was added to the mixture, and homogeneous ternary mixtures were obtained. After that, the mixtures were immediately degassed at 80 °C under vacuum and were cured at this temperature for 15 h. After curing, the plaques were slowly cooled to room temperature, demolded, and postcured for 2 h at 160 °C under vacuum. Though not shown, thermogravi-

10.1021/ma8022553 CCC: $40.75
Published on Web 04/16/2009

metric analysis (TGA) confirmed the incorporation of 1 wt % of the TiO_2 into inorganic/organic thermosetting materials.

Techniques. We analyzed the final morphologies of the inorganic/organic nanostructured thermosetting materials in tapping mode by using atomic force microscopy (AFM) (Nanoscope IIIa Multimode and Nanoscope IVa Dimension 3100 both from Digital Instruments) equipped with an integrated silicon tip/cantilever having a resonance frequency of ~300 kHz. Electric force microscopy (EFM) was successfully employed to visualize the dispersion of conductive dioxide titanium nanoparticles. Measurements were performed in the lift mode (lift height was 180 nm) under ambient conditions, and AFM was equipped with an integrated Co/Cr-coated MESP tip with a resonance frequency of ~75 kHz. We detected the secondary imaging mode derived from tapping mode that measures electric field gradient distribution above the sample surface by applying a voltage to the cantilever tip. To obtain repeatable results of the investigated materials, we scanned different regions of the specimens. Similar images were obtained, thus demonstrating the reproducibility of the AFM and EFM images. We obtained the flat surfaces of the modified thermosetting systems by cutting with a diamond knife using a Leica Ultracut R ultramicrotome.

A Tecnai G2 20 twin microscope operated at 200 kV accelerating voltage was used for TEM measurements. We prepared TEM samples by using an ultramicrotome (Leica Ultracut R) equipped with a diamond knife. Moreover, TEM samples were stained with RuO_4 vapor for 4 min to enhance contrast between the HBC liquid crystal and the PS-block/epoxy regions.

Different methods such as differential scanning calorimetry (DSC, Mettler Toledo DSC 822) and transmission optical microscopy (TOM, Nikon Eclipse E600) equipped with hot stage (Mettler FP 82HT) were used to characterize inorganic/organic nanostructured thermosetting materials and the same epoxy-modified systems without TiO_2 nanoparticles.

Results and Discussion

Taking into account our recently published papers,[25−30] thermosetting materials modified with PSEO block-copolymers-dispersed HBC liquid crystals are of great interest because of their thermo- and electroresponsive behavior. These materials can switch from the opaque to the transparent state (OFF/ON state) because curing the reaction-induced microphase separation of the PS block leads to HBC microphase separation within PS-block domains, and simultaneously, the HBC phase maintains properties of the neat nematic LC. As is well-known, conductive nanoparticles dispersed in low-molecular-weight liquid crystal matrices lead to large electro-optic effects.[7−12] Consequently, the introduction of TiO_2 nanoparticles to a thermoresponsive thermosetting system modified with PSEO block-copolymer-dispersed HBC liquid crystals can open up the possibility of designing novel materials with very interesting potential applications. A representative AFM phase image of the 1 wt % TiO_2−15 wt % PSEO−40 wt % HBC−(DGEBA/MXDA) is shown in Figure aI. Neither titanium oxide nanoparticles nor their agglomerates are detected on the ultramicrotomed surface. Furthermore, the comparison of the final morphology of this system to the same system without titanium dioxide nanoparticles (Figure 1b) suggests that nanoparticles are confined within HBC/PS-nanodomains that are microphase-separated from the PEO-block/HBC/epoxy-rich phase. The average size of the microphase-separated domains decreases from 40 to 75 nm to 40 to 55 nm for epoxy systems modified with 1 wt % TiO_2−15 wt % PSEO−40 wt % HBC and 15 wt % PSEO−40 wt % HBC, respectively. Here it should be also pointed out that the brighter continuous regions in the AFM phase images are ascribed to the epoxy-cured network, which is partially miscible with the PEO block and HBC phase,[26,28−30] whereas the dark areas correspond to HBC/PS-rich microdomains, probably with TiO_2 nanoparticles included. TiO_2 nanoparticles are possibly not detected because they are covered by the HBC phase because liquid crystal acts as surfactant, which seems to be more reasonable taking into account that the difference between microphase-separated domains of thermosetting materials modified with and without TiO_2 nanoparticles is around 20 nm, similar to the size of the incorporated rutile nanoparticles.

Moreover, the corresponding TEM image of 1 wt % TiO_2−15 wt % PSEO−40 wt % HBC−(DGEBA/MXDA), Figure aII, confirms the morphology detected by AFM, indicating that the average size of the microphase-separated domains increases to 40−75 nm. Indeed, the introduction of TiO_2 nanoparticles increases the size of microphase-separated HBC/PS-rich microdomains around 20 nm with respect to the system without nanoparticles. Additionally, TEM allows us to deduce that microphase-separated domains consist of two different separated phases with a well-defined interface between them (inset of the Figure aII). Because the TEM sample was stained with RuO_4, the dark region corresponds to the PS phase and the light region corresponds to HBC liquid crystal.[31] The average size of the lightest region inside the microphase-separated domains is 20−40 nm. Taking this and the fact that in the TiO_2(HBC/PSEO) system the inorganic nanoparticles are surrounded by liquid crystal into account,[32] it seems that rutile TiO_2 nanoparticles phase-separate with HBC liquid crystal inside the PSEO/HBC rich phase[29,30] located close to the interface with the HBC/epoxy matrix (inset of the Figure aII).

To verify the segregation of TiO_2 nanoparticles in the HBC/PS-block phase, we performed two different sample treatments. In the first one, the sample was irradiated by UV light of 254 nm (XX-15S, UPS) at room temperature for 3 h to remove the HBC/PS-block organic phase behind the titanium dioxide domains. In Figure 1c, the morphology of the 1 wt % TiO_2−15 wt % PSEO−40 wt % HBC-(DGEBA/MXDA) epoxy blend after 3 h of UV treatment is shown. This time has been chosen because after 3 h of exposure, any significant changes on the sample surface were able to be detected. In Figure 1c, the AFM phase image shows the brightest well-distributed spontaneously arranged domains of TiO_2 (well-detected in the 3D inset of the Figure 1c) in the grayest epoxy network-rich matrix. The size of the brightest domains is around 19−32 nm while taking into account the fact that rutile TiO_2 nanoparticles are commercially 20 nm in size, which confirms that these well-dispersed segregated domains can be attributed to TiO_2 nanoparticles.

The second treatment to verify the segregation of TiO_2 nanoparticles was carried out using electrostatic force microscopy (EFM). The voltage was continuously applied to the ultramicrotomed sample surface of the 1 wt % TiO_2−15 wt % PSEO−40 wt % HBC−(DGEBA/MXDA) epoxy blend in which the sample surface had been continuously scanned for 3 h with the 12 V applied to the EFM tip. A representative AFM phase image of a 12 V EFM-tip-treated sample is shown in Figure 1d. Three different phases indicated by different scale colors can be easily distinguished in the AFM phase image. The strong dark separated domains can be attributed to the HBC/PS-block phase with the average width of domains being around 25−50 nm. Additionally, the brightest spherical domains with an average size between 16 and 30 nm can be clearly recognized as TiO_2 nanoparticles, which are spontaneously arranged as nanodots consisting of 5−12 nanoparticles that are generally positioned in the interface between the epoxy-modified rich phase and the HBC/PS-block phase. Here it should be pointed out that if one sums the average sizes of both the brightest rutile TiO_2 nanoparticles and the strong dark microphase-separated HBC/PS-block domains in Figure 1d, then the value corresponds to the average size of one unique dark microphase-separated domain in Figure 1a. As expected, taking both this comparison and literature[7−12] into account, TiO_2 nanoparticles are covered

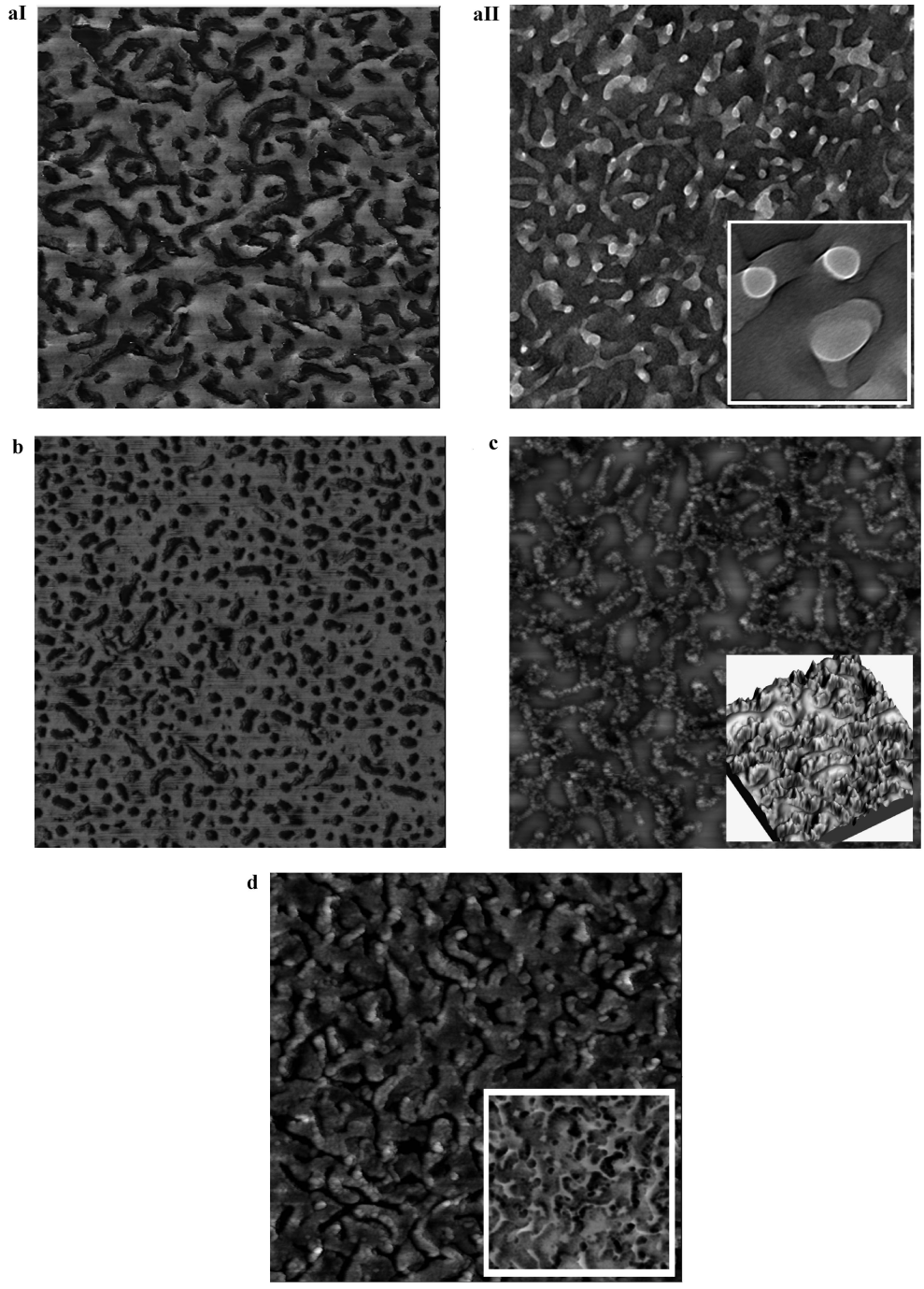

Figure 1. (aI) TM-AFM phase image ($2 \times 2\ \mu m^2$) of 1 wt % TiO_2−15 wt % PSEO−40 wt % HBC−(DGEBA/MXDA) epoxy system. (aII) TEM image ($2 \times 2\ \mu m^2$) of 1 wt % TiO_2−15 wt % PSEO−40 wt % HBC−(DGEBA/MXDA) epoxy system; inset: a higher magnification detail. TM-AFM phase images ($2 \times 2\ \mu m^2$) of (b) 15 wt % PSEO−40 wt % HBC−(DGEBA/MXDA) epoxy system; (c) 1 wt % TiO_2−15 wt % PSEO−40 wt % HBC−(DGEBA/MXDA) epoxy system after 3 h of UV light exposure; inset: 3D image; (d) 1 wt % TiO_2−15 wt % PSEO−40 wt % HBC−(DGEBA/MXDA) epoxy system after 3 h of applying 12 V by using EFM tip; inset: negative image.

by the HBC liquid crystal phase, and consequently, the reaction-induced microphase-separation of the HBC/PS-block leads to segregation of TiO_2 nanoparticles covered by the HBC phase within. Additionally, well-organized nanodots (black domains in the negative image) formed by single rutile nanocrystals located along the microphase-separated HBC/PS-block domains are easily distinguished in the negative image of the inset of Figure 1d.

At this point, the still open question is whether the HBC liquid crystal acts as a surfactant and provokes the spontaneous arrangement in the form of the nanorodlike structure of the well-dispersed TiO_2 nanoparticles under the used preparation conditions or whether this is also the influence of the PSEO block copolymers, which could confine titanium dioxide nanoparticles in the microphase-separated PS-block phase. To verify this, the 1 wt % TiO_2−15 wt % PSEO−(DGEBA/MXDA) epoxy blend was prepared under the same conditions. The morphology of this system is shown in Figure 2a. Two different microphase-separated domains can be easily distinguished. The dark one corresponds to the microphase-separated PS block, and the brightest domains clearly correspond to microphase-separated rutile TiO_2 nanoparticles preferentially located close to the interface between the PS-block and the epoxy matrix. To be certain that those spherical brightest domains corresponded to TiO_2 nanoparticles, we mapped EFM images by applying 12 V to the EFM tip. As can be recognized in Figure 2b, the brightest

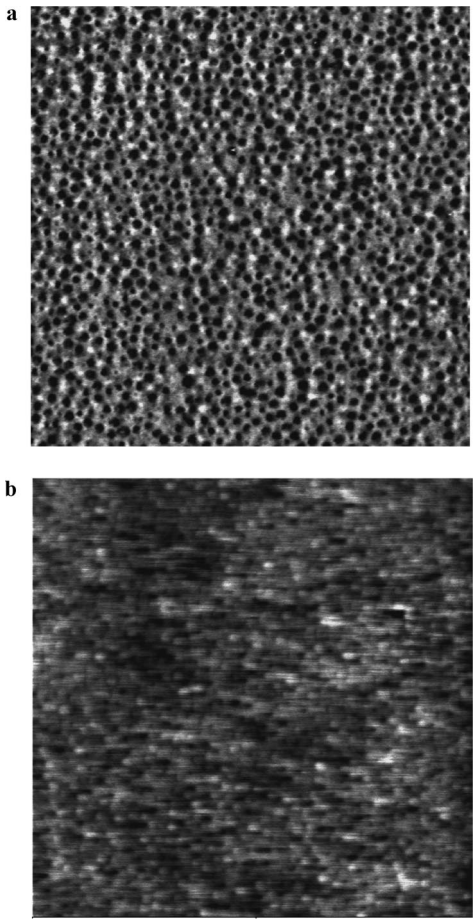

Figure 2. (a) TM-AFM phase image ($2 \times 2\ \mu m^2$) of 1 wt % TiO_2−15 wt % PSEO−(DGEBA/MXDA) epoxy system. (b) EFM phase image of 1 wt % TiO_2−15 wt % PSEO−(DGEBA/MXDA) epoxy system in lift mode applying 12 V.

domains can respond to the application of voltage, which, taking into account that the PS-block phase in the PSEO-(DGEBA/MXDA) epoxy blend does not show any signals when voltage is applied,[28] confirms that these domains can be attributed to TiO_2 nanoparticles and that these nanoparticles maintain the conductive properties in the inorganic/organic thermosetting materials. These results prove that the microphase-separated HBC is responsible for the spontaneous arrangement of the conductive rutile TiO_2 nanoparticles into the HBC/PS-block phase and that nanodots are located in the interface with epoxy-rich phase.

Differential scanning calorimeter (DSC) measurements confirm that the HBC phase in the 1 wt % TiO_2−15 wt % PSEO−40 wt % HBC−(DGEBA/MXDA) epoxy blend maintains the properties of the neat HBC liquid crystal because this phase possesses a nematic−isotropic transition during the heating/cooling process, as is indicated by the arrows in the inset of Figure 3. Moreover, as expected, these materials can switch from the completely opaque to the transparent state just by applying temperature gradients (digital images insets in Figure 3). Comparisons between the DSC endo- and exothermic peaks for 1 wt % TiO_2−15 wt % PSEO−40 wt % HBC−(DGEBA/MXDA) epoxy blend and the neat HBC (Figure 3) indicate a significant decrease of the crystalline in the inorganic/organic thermosetting materials, which, simultaneously with the ability of switching from the opaque to the transparent state, leads to materials with high contrast between opaque and transparent during the nematic−isotropic transition.

Finally, it should be pointed out that the obtained results clearly prove that the spontaneous arrangement of TiO_2 nanoparticles provoked by the HBC phase in inorganic/organic thermosetting materials modified by PSEO is an effective method for the preparation of novel multiphase thermoresponsive nanostructured materials based on thermosetting matrices. These materials can find many different applications in different fields of nanotechnology taking into account that they maintain specific properties of both nematic liquid crystals and conductive, photo-optically active rutile TiO_2 nanoparticles. Further examination of these and related systems is currently underway to quantify the ratio between low-molecular-weight nematic liquid crystals, rutile TiO_2 nanoparticles, and amphiphilic block copolymers necessary to generate these multiphase thermo- and electroresponsive nanostructured hybrid inorganic/organic thermosetting materials with high contrast ratio.

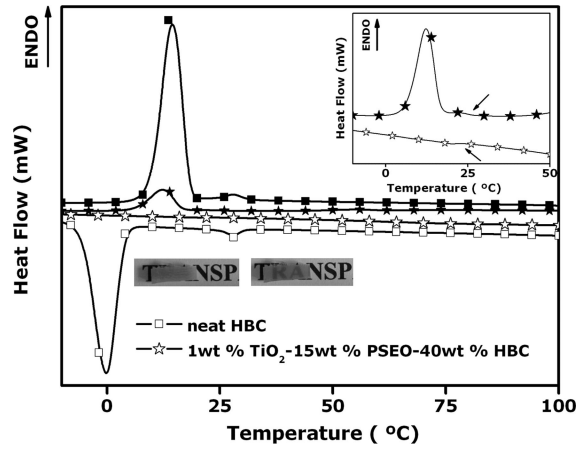

Figure 3. DSC thermograms of (-■-/-□- heating/cooling) neat HBC liquid crystal and (-★-/-☆- heating/cooling) 1 wt % TiO_2−15 wt % PSEO−40 wt % HBC−(DGEBA/MXDA) epoxy system; inset: details of DSC thermograms of the 1 wt % TiO_2−15 wt % PSEO−40 wt % HBC−(DGEBA/MXDA) epoxy system. Transparency of this blend at 16 °C (digital image on the left) and at room temperature (digital image on the right).

Conclusions

TiO_2nanoparticles were successfully dispersed in a multiphase nanostructured thermosetting system modified with PSEO block-copolymer-dispersed HBC liquid crystals. Arrays of 20 nm size nanoparticles along HBC/PS-block microphase-separated domains are spontaneously developed because in this system, the HBC phase acts as surfactant for TiO_2 nanoparticles. The designed materials maintain the properties of both the nematic liquid crystals, because they are able to switch from the opaque to the transparent state by applying thermal gradients, and TiO_2 nanoparticles, because they respond to the voltage applied to the EFM tip. This results in the generation of novel hybrid inorganic/organic materials based on thermosetting matrices for potential nano-optoelectronic applications.

Acknowledgment. Financial support from Basque Country Governments in the frame of Grupos Consolidados (IT-365-07), inanoGUNE, and SAIOTEK (S-PE07UN39) projects is gratefully acknowledged. We also thank the Spanish Ministry of Education and Science for MAT2006-06331:FUNAN.

References and Notes

(1) Darling, S. B. *Surf. Sci.* **2007**, *601*, 2555–2561.
(2) Medintz, I. L.; Clapp, A. R.; Melinger, J. S.; Deschamps, J. R.; Mattoussi, H. *Adv. Mater.* **2005**, *17*, 2450–2455.
(3) Zhang, Q.; Gupta, S.; Emrick, T.; Russell, T. P. *J. Am. Chem. Soc.* **2006**, *128*, 3898–3899.

(4) Steunou, N.; Förster, S.; Florian, P.; Sanchez, C.; Antonietti, M. *J. Mater. Chem.* **2002**, *12*, 3426–3430.
(5) Manias, E. *Nat. Mater.* **2007**, *6*, 9–11.
(6) Qi, H.; O'Neil, J.; Hegmann, T. *J. Mater. Chem.* **2008**, *18*, 374–380.
(7) In, I.; Jun, Y.-W.; Kim, Y. J.; Kim, S. Y. *Chem. Commun.* **2005**, *6*, 800–801.
(8) Jeng, S. Ch.; Kuo, Ch. W.; Wang, H. L.; Liao, Ch. Ch. *Appl. Phys. Lett.* **2007**, *91*, 061112/1–061112/3.
(9) Kaczmarek, M.; Buchnev, O.; Nandhakumar, I. *Appl. Phys. Lett.* **2008**, *92*, 103307/1–103307/3.
(10) Payne, J. C.; Thomas, E. L. *Adv. Funct. Mater.* **2007**, *17*, 2717–2721.
(11) da Cruz, C.; Sandre, O.; Cabuil, V. *J. Phys. Chem. B* **2005**, *109*, 14292–14299.
(12) Hegmann, T.; Qi, H.; Marx, V. M. *J. Inorg. Organomet. Polym. Mater.* **2007**, *17*, 483–508.
(13) Hillmyer, M. A.; Lipic, P. M.; Hajduk, D. A.; Almdal, K.; Bates, F. S. *J. Am. Chem. Soc.* **1997**, *119*, 2749–2750.
(14) Lipic, P. M.; Bates, F. S.; Hillmyer, M. A. *J. Am. Chem. Soc.* **1998**, *120*, 8963–8970.
(15) Dean, J. M.; Lipic, P. M.; Grubbs, R. B.; Cook, R. F.; Bates, F. S. *J. Polym. Sci., Part B: Polym. Phys.* **2001**, *39*, 2996–3010.
(16) Ritzenthaler, S.; Court, F.; David, L.; Girard-Reydet, E.; Leibler, L.; Pascault, J. P. *Macromolecules* **2002**, *35*, 6245–6254.
(17) Ritzenthaler, S.; Court, F.; David, L.; Girard-Reydet, E.; Leibler, L.; Pascault, J. P. *Macromolecules* **2003**, *36*, 118–126.
(18) Serrano, E.; Martin, M. D.; Tercjak, A.; Pomposo, J. A.; Mecerreyes, D.; Mondragon, I. *Macromol. Rapid Commun.* **2005**, *26*, 982–985.
(19) Serrano, E.; Tercjak, A.; Kortaberria, G.; Pomposo, J. A.; Mecerreyes, D.; Mondragon, I. *Macromolecules* **2006**, *39*, 2254–2261.
(20) Ocando, C.; Serrano, E.; Tercjak, A.; Peña, C.; Kortaberria, G.; Calberg, C.; Grignard, B.; Jerome, R.; Carrasco, P. M.; Mecerreyes, D.; Mondragon, I. *Macromolecules* **2007**, *40*, 4068–4074.
(21) Meng, F.; Zheng, S.; Li, H.; Liang, Q.; Liu, T. *Macromolecules* **2006**, *39*, 5072–5080.
(22) Maiez-Tribut, S.; Pascault, J. P.; Soule, E. R.; Barrajo, J.; Williams, R. J. J. *Macromolecules* **2007**, *40*, 1268–1273.
(23) Xu, Z.; Zheng, S. *Macromolecules* **2007**, *40*, 2548–2558.
(24) Meng, F.; Zhiguang, X.; Zheng, S. *Macromolecules* **2008**, *41*, 1411–1420.
(25) Tercjak, A.; Serrano, E.; Mondragon, I. *Polym. Adv. Technol.* **2006**, *17*, 835–840.
(26) Tercjak, A.; Serrano, E.; Mondragon, I. *Macromol. Rapid Commun.* **2007**, *28*, 937–941.
(27) Tercjak, A.; Serrano, E.; Garcia, I.; Ocando, C.; Mondragon, I. *Acta Mater.* **2007**, *55*, 6436–6443.
(28) Tercjak, A.; Garcia, I.; Mondragon, I. *Nanotechnology* **2008**, *19*, 155607/1–155607/5.
(29) Tercjak, A.; Serrano, E.; Garcia, I.; Mondragon, I. *Acta Mater.* **2008**, *56*, 5112–5122.
(30) Tercjak, A.; Mondragon, I. *Langmuir* **2008**, *24*, 11216–11224.
(31) Hayakawa, T.; Horiuchi, S.; Shimizu, H.; Kawazoe, T.; Ohtsu, M. *J. Polym. Sci., Part A: Polym. Chem.* **2003**, *40*, 2406–2424.
(32) Tercjak, A.; Gutierrez, J.; Ocando, C.; Peponi, L.; Mondragon, I. Thermo-responsive inorganic/organic hybrids based on conductive TiO_2 nanoparticles embedded in poly(styrene-*b*-ethylene oxide) block copolymer dispersed liquid crystals. *Acta Mater.*, sent for publication.

MA8022553